Materials Today Advances 5 (2020) 100047

Contents lists available at ScienceDirect

Materials Today Advances

journal homepage: www.journals.elsevier.com/materials-today-advances/

Transport in nanopores and nanochannels: some fundamental challenges and nature-inspired solutions

Y.A. Perez Sirkin [a], M. Tagliazucchi [a], I. Szleifer [b,*]

[a] INQUIMAE-CONICET and DQIAQF, University of Buenos Aires, School of Sciences, Ciudad Universitaria, Pabellón 2, Ciudad Autónoma de Buenos Aires, C1428EHA, Argentina

[b] Department of Biomedical Engineering, Department of Chemistry and Chemistry of Life Processes Institute, Northwestern University, Evanston, IL, 60208, USA

ARTICLE INFO

Article history:
Received 13 September 2019
Received in revised form
6 December 2019
Accepted 11 December 2019
Available online 15 January 2020

Keywords:
Ion transport
Bioinspiration
Ion selectivity
Nuclear pore complex
Theory

ABSTRACT

The field of solid-state nanopores and nanochannels has grown exponentially in the past five years. Recent advances have greatly broadened the spectrum of available gating stimuli, expanded applications in sensing, energy conversion, and separation science, and improved our understanding of the mechanisms that govern ion transport in nanometer-sized channels and pores. Despite these impressive achievements, there still exists very challenging (and very exciting) research directions. This review focuses on three of these directions: i) ion selectivity: is it possible to construct channels that discriminate one type of ion from others with the same charge and similar size? ii) Integration with chemical networks: how can chemical networks, which are ubiquitous in living organisms, be integrated with pores and channels to enable new functions and enhance current applications? iii) Transport of cargoes larger than ions: is it possible to achieve selective and stimuli-gated transport of macromolecules and nanoparticles through synthetic pores? A brief analysis of biological channels and pores demonstrates that nature had evolved fascinating solutions for these three problems that may serve as a source of inspiration.

1. Introduction

In a previous review of the transport mechanisms through nanopores and nanochannels [1], we argued that synthetic channels and pores will probably never mimic the exact transport behaviors of their biological counterparts. However, these mechanisms and the functions that they enable serve as a source of inspiration for researchers aiming to expand the capabilities of synthetic nanofluidic devices. It should be noted that the creative impulses behind scientific advances in this field are not always inspired by biology; nevertheless, we believe that comparison with biological systems is always fruitful. This comparison allows us to understand the advantages and limitations of synthetic systems and unveils new directions for further improvement.

In many performance criteria, synthetic pores and channels have already outclassed biological systems. For example, in recent years, the number of stimuli that can gate the conductance of synthetic channels and pores has exponentially expanded. These stimuli now include alkaline cations [2–5], heavy metals [6–8], anions [9,10], monosaccharides [11,12], DNA [13,14], aminoacids [15,16], gases [17,18], proteins [19], pH [20–25], light [26–29], and changes of pressure [30], temperature [31,32], and membrane potential [33,34], among others. This rich spectrum of chemical and physical stimuli rivals and even surpasses that of biological channels. Another aspect where synthetic pores and channels have a performance comparable to or better than that of biological ones is current rectification. Fine control over the shape and charge distribution in asymmetric shaped nanochannels [35–37] and bipolar diodes [38–41] have yielded devices with very high rectification ratios. For example, by combining shape and charge asymmetries, Vlassiouk and Siwy demonstrated a rectification ratio of ~25 in conical bipolar diodes under physiological conditions (pH 7 and $I = 0.1$ M), which is similar to the values measured for inward rectifier potassium channels [42]. Even higher rectification ratios can be achieved in synthetic asymmetric membranes with multiple channels (up to 1000) [43] or in single synthetic asymmetric nanopores with confined polyelectrolyte complexes (up to 2000) [44].

* Corresponding author.
E-mail address: igalsz@northwestern.edu (I. Szleifer).

https://doi.org/10.1016/j.mtadv.2019.100047

years, the number of stimuli that can gate the conductance of

* Corresponding author.

rectifier potassium channels [42]. Even higher rectification ratios can be achieved in synthetic asymmetric membranes with multiple channels (up to 1000) [43] or in single synthetic asymmetric nanopores with confined polyelectrolyte complexes (up to 2000)

Despite the fact that in many aspects the performance of synthetic channels and pores now surpasses that of their biological analogs, synthetic devices still lag behind natural channels in many other important criteria. In this review, we will focus on three of these aspects and challenges, namely:

i) Ion selectivity: can we construct channels and pores that selectively transport one ion over another one with similar charge and size? (e.g., Li^+ over Na^+ and K^+)
ii) Signal amplification: can we enhance the detection limits of nanochannel-based sensors by coupling them to chemical-amplification reaction cascades?
iii) Transport of cargoes larger than ions: can we construct channels or pores that selectively allow the passage of some specific cargoes (e.g., nanoparticles or proteins) while blocking others? Alternatively, can we construct channels that can be selectively opened/closed for large molecules or particles, but always remain open for small molecules and ions?

These three problems are of course just a selection of the many challenges in nanochannel science for which biology may serve as a source of inspiration. The goal of this review is to critically examine recent work in these interesting areas, to compare the underlying mechanisms to biological processes, and to discuss how natural channels and pores may inspire further approaches to advance in these areas. It should be noted that we do not intend to comprehensively review the field of bioinspired nanochannels and nanopores, which have quickly grown in recent years. We refer the reader to some recent reviews [45–54] for a systematic and complete approach to the field.

2. Ion selectivity: filtering ions by size and charge

The scientific community is investing great effort in the development of new technologies to selectively remove or concentrate certain ions from solution. Such technologies hold the promise of economic, efficient, and environmentally friendly water desalination methods, e.g., the removal of salt from seawater to obtain fresh water. They also promise to revolutionize the extraction of high purity lithium salts from salt-lake brines for their use in lithium batteries [55]. Nanopore materials are promising candidates to achieve these goals [56].

Interestingly, nature has devised ways to separate ions from water or other ions. The water-selective channels called aquaporins (AQP) are prototypical examples of efficient ion/water separation in biology [57]. These systems allow water to flow through biological membranes, but hinder the transport of ions, in particular, protons. Water molecules transit through the pore in a single row, maintaining a distance between water molecules that is large enough to avoid the formation of hydrogen bonds. The shape of AQP1 exhibits a wide opening at the membrane surface and a constriction in the center that results in a high dielectric barrier. This barrier repels ions and grants passage to neutral water molecules [57]. Although AQP block all ions, there are important biological channels that selectively allow the passage of one type of ion and reject the others. For example, KcsA potassium channels show a K^+/Na^+ selectivity ratio of 1000–10000 for a transport rate of 10^8 K^+ ions/(s.channel) [58,59]. Sodium channels are usually less selective than potassium ones, for example the epithelial Na^+ channel (ENaC), which is one of the most selective sodium channels, has a Na^+/K^+ selectivity ratio of 100–500 [59].

The efficiency of ion separation of synthetic nanochannels is generally evaluated in terms of their ability to selectively transport one ion over other (ion selectivity) and of the transport rate of the ion of interest (ion permeability). The selectivity can be modulated by different factors, such as the dimensions of the nanochannel and the electrostatic and non-electrostatic ion-wall interactions [23,60–63]. When the radius of the nanopore is less than the radius of the hydrated ion, ion selectivity is controlled by channel's radius and the transport rate is controlled by the dehydration or partial dehydration (e.g., loss of the second hydration shell) of the ion at the entrance of the pore. On the other hand, when the radius is larger than the size of the hydrated ion, then the transport rate tends to that expected from the bulk mobility and the interactions between the ion and channel walls are responsible for ensuring ion selectivity (note, however, that in this case the selectivity is generally lower than when the channel radius is smaller than the ion). Wang et al. [63] reported an interesting molecular dynamics simulation study that exemplifies the competition between the two selectivity mechanisms discussed above (dehydration effects vs electrostatic interactions). This work showed that the Li^+/Mg^{2+} selectivity can be tuned by increasing the surface charge of carbon nanotubes.

Several synthetic nanopores have been developed to obtain ion selectivity and permeability using different materials such as graphene, Nafion, or metal–organic frameworks (MOFs). We briefly discuss below a few selected examples, where the ion selectivity is achieved by different mechanisms. One important example, presented by Zhang et al. [64], involves a MOF denoted as ZIF-8 that was deposited on an anodic aluminum oxide support (AAO) assisted by graphene oxide (GO). The resulting ZIF-8/GO/AAO membrane has angstrom-sized windows (∽3.4 Å) that act as ion-selective filters and nanometer-sized cavities (∽11.6 Å) that allow fast ion transport (see Fig. 1A.ii). The selectivity ratios reported for Li^+/Rb^+, Li^+/K^+, and Li^+/Na^+ were 4.6, 2.2, and 1.4, respectively (see Fig. 1A.i). These ion selectivities were mainly ascribed to the sub-angstrom difference in the partially dehydrated ionic diameters of the alkali ions.

In another example of ion selectivity in synthetic systems, Wen et al. [65] presented a polymer polyethylene terephthalate (PET) membrane with subnanometer channels of radii ∽0.3 nm and a thickness of 12 μm. The inner surface of the channels has charged carboxylate groups that confer the system a cation/anion selectivity of up to 10^8, an alkali metal ion/heavy ion selectivity of up to 10^6, and an alkali metal ion/alkaline earth metal ion selectivity of up to 10^3. The high selectivity of cations over anions was ascribed to the interaction of the ions with the carboxylate groups, as demonstrated by the fact that the transport rate of sodium cations significantly dropped when the wall was neutralized by lowering the pH of the solution. This charge-based selectivity mechanism (unipolar transport) is well-known and has been extensively described in the literature [66]. Interestingly, this effect cannot explain the high selectivity observed between different types of cations. Molecular dynamics simulations suggested that the selectivity between different types of cations results from dehydration effects. Although the selectivity is very high in this system, it has slow transport rates. In a follow-up work (see Fig. 1C), the same group reported a new configuration of the material with channels of radius ∽0.5 nm and a thickness of 2 μm that shows a significant increase in permeability, but also a decrease in the ionic selectivity for alkaline metal ions [64].

Guo et al. [62] provided another interesting example of ion selectivity. The authors constructed a polystyrene-sulfonate-threaded MOF (PSS@HKUST-1-6.7), see Fig. 1B.ii. This material exhibits selectivity ratios for Li^+/Na^+, Li^+/K^+, and Li^+/Mg^{2+} of 35, 67, and 1815, respectively, Fig. 1B.i. The very high selectivity was not attributed to the size of the hydrated or dehydrated ions but rather to the affinity of the cation to the sulfonate groups in the membrane. The corresponding binding affinities of Li^+, Na^+, and K^+

selectivity ratio of 1000–10000 for a transport rate of 10^8 K^+ ions/(s.channel) [58,59]. Sodium channels are usually less selective than potassium ones, for example the epithelial Na^+ channel (ENaC), which is one of the most selective sodium channels, has a Na^+/K^+ selectivity ratio of 100–500 [59].

Guo et al. [62] provided another interesting example of ion selectivity. The authors constructed a polystyrene-sulfonate-threaded MOF (PSS@HKUST-1-6.7), see Fig. 1B.ii. This material exhibits selectivity ratios for Li^+/Na^+, Li^+/K^+, and Li^+/Mg^{2+} of 35, 67, and 1815, respectively. Fig. 1B.i. The very high selectivity was not

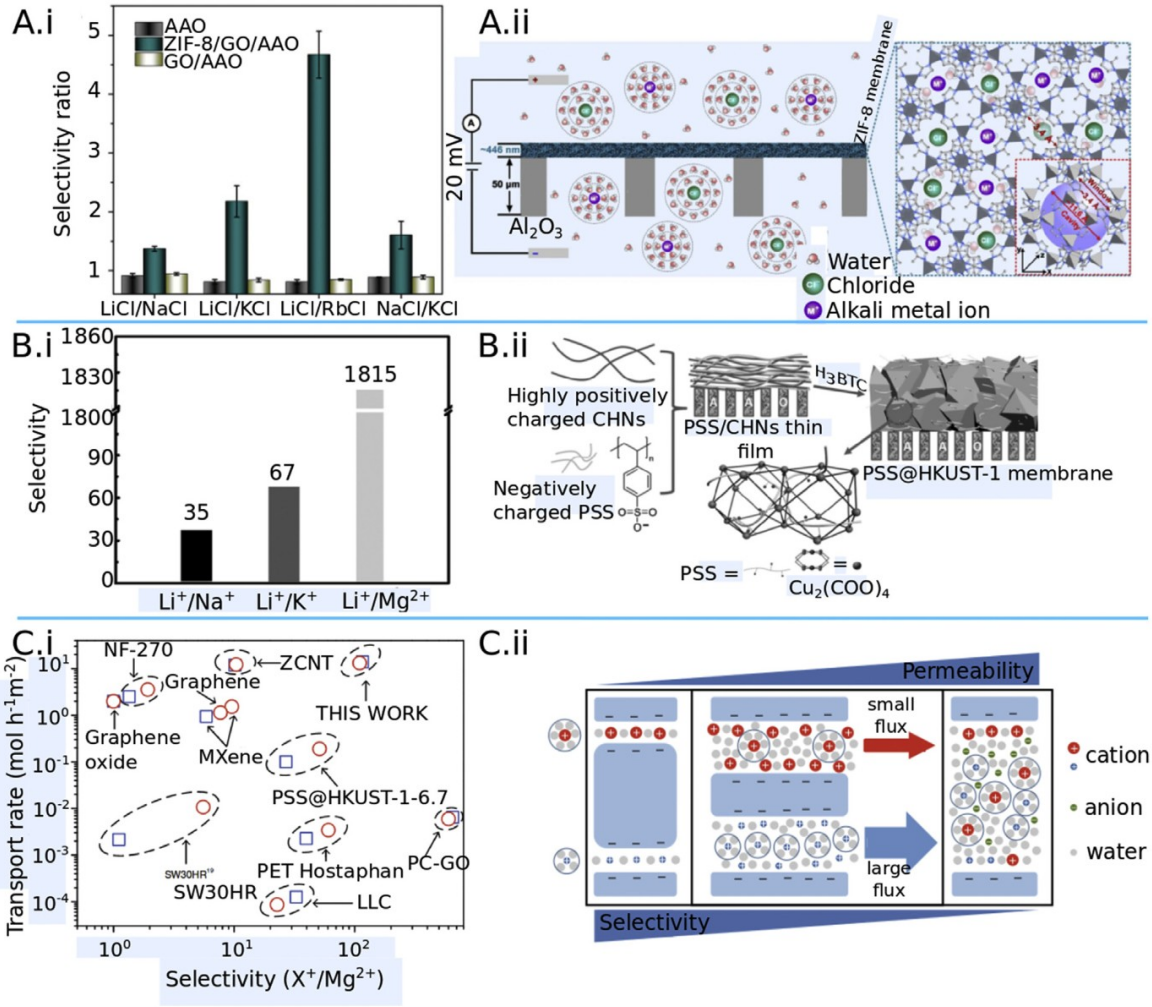

Fig. 1. Examples of different nanopore systems that exhibit selectivity between ions of the same charge. A.i) Ion selectivity ratios of the AAO support, ZIF-8/GO/AAO membrane, and GO/AAO membrane. A.ii) Schematic representation of the ZIF-8/GO/AAO membrane. The inset shows the crystal structure of ZIF-8. Reproduced and adapted with permission from Ref. [71]. Copyright 2018 The Authors, some rights reserved; exclusive licensee American Association for the Advancement of Science. B.i) Ion selectivity ratios of PSS@HKUST-1-6.7. B.ii) Schematic representation of the preparation of PP-threaded HKUST-1 membranes. CHNs = copper hydroxide nanostrands. AAO = anodic alumina. Reproduced and adapted with permission from Ref. [62]. Copyright 2016 Wiley-VCH Verlag GmbH & Co. KGaA. C.i) Transport rates vs. K^+/Mg^{2+} (blue squares) and Na^+/Mg^{2+} (red circles) selectivity ratios for various nanopore membranes. C.ii) Schematic representation of the effect of the pore radius on ion transport through a negatively charged nanopore. Left panel: the size of the nanopore is smaller than the hydration radius of the ions. Therefore, partial or total dehydration is the predominant mechanism, and then high selectivity, but low permeability is expected. In the opposite case, right panel, the nanopore radius is much larger than the ion radius; the nanopore shows high permeability and low selectivity. In an intermediate case, center panel, it is possible to obtain high permeability and high selectivity if the interaction with the pore surface is different for each ion type. Reproduced and adapted with permission from Ref. [64]. Copyright 2018 Nature Publishing Group.

(normalized by Li^+) are 1.0, 1.98, and 2.90, respectively. Therefore, as the binding affinity increases, the cation-sulfonate condensation is facilitated and the ionic conductance decreases. In the particular case of Mg^{2+}, the high selectivity is attributed not only to the high affinity of the sulfonate for Mg^{2+} (3.18), but also to the size of hydrated Mg^{2+} (0.86 nm), which is comparable with the size of the pore entrance in the MOF (0.9 nm). The combined effects of the size of the pore and its binding affinity contribute to the outstanding Li^+/Mg^{2+} selectivity ratio of 1815.

Crown-ethers, known for their ability to selectively bind alkaline cations, are interesting modifiers for the preparation of nanopores and nanochannels with high ionic selectivity. Acar et al. prepared a nanopore in a silicon-nitride support, whose inner surface was modified with 4′-aminobenzo-18-crown-6 ether and DNA single strands (ssDNA) were grafted at one of the pore entrances. This system displays high K^+/Na^+ selectivity ratios of up to 84. The high selectivity is attributed to the facilitated transport of potassium ions through the crown ether, whereas the ssDNA plays the role of a cation filter [67]. Chen et al. used molecular dynamic simulations to study a stack of graphene layers with nanopores resembling 18-crown-6. This stack selectively transported K^+ over Na^+. The authors evaluated different parameters such as the number of layers and the distance between them to increase the K^+/Na^+ selectivity, reaching a maximum value close to 3 [68].

Balme et al. [69,70] proposed an alternative approach to construct ion-selective pores, where a biological ion channel, Gramicidin A (GA), is confined into cylindrical nanopores in a solid-state membrane. This synthetic system reproduces some behaviors of the ion-channel in its native environment, for example the NaCl/KCl diffusion coefficient ratio. However, the membrane cannot block divalent cations and chloride, which was attributed to the lack of the head-to-head conformation that is observed when GA is

Crown-ethers, known for their ability to selectively bind alkaline cations, are interesting modifiers for the preparation of nanopores and nanochannels with high ionic selectivity. Acar et al. prepared a nanopore in a silicon-nitride support, whose inner

construct ion-selective pores, where a biological ion channel, Gramicidin A (GA), is confined into cylindrical nanopores in a solid-state membrane. This synthetic system reproduces some behaviors of the ion-channel in its native environment, for example the NaCl/

inserted into a lipid environment. One exceptional property of this biological/artificial system is that it is permeable to K^+ and Na^+, but totally impermeable to H^+. This result contrasts the behavior of GA in nature, where the H^+ transport is faster than that of other monovalent cations [70].

3. Signal amplification

Most gating stimuli mentioned in the Introduction modulate the conductance of channels by directly binding to their inner surface, which affects the channel cross-sectional area, its surface charge, or both. However, the regulation of biological channels and pores is significantly more complex and less straightforward than that of synthetic channels. Living organisms use signaling pathways to coordinate a myriad of simultaneous chemical processes, including transport through channels and pores. These signaling systems constitute complex chemical networks that use control mechanisms such as feedback loops, allosteric effects, and chemical amplification. There are many examples of the integration of biological channels into chemical networks. For example, feedback loops, a mechanism that involves the inhibition of a process by its product, maintain regulation and hemostasis in biological networks. In the case of ion channels, feedback is crucial to regulate the intracellular concentration of Ca^{2+} ions, for example, by Ca^{2+}-induced deactivation of some specific voltage-gated Ca channels (CaV1.2) [72].

Another recurrent strategy in biochemical networks is signal amplification. This strategy is crucial in the chemical mechanism responsible for vision, which comprises a complex signaling cascade that ultimately results in the inactivation of an ion channel. Rhodopsin is a membrane protein constituted by the protein opsin and a covalently bound chromophore known as retinal [73]. Photon absorption by retinal triggers a *cis-trans* isomerization that causes a conformational change in the protein, which, in turn, activates a coupled G protein. The G protein activates a phosphodiesterase that cleaves cGMP (cyclic guanosine monophosphate) [74]. The loss of cGMP causes cGMP-gated Na^+ ion channels to close, which finally results in a neuronal action potential. Noteworthy, each opsin can activate over a hundred G proteins; each of these proteins activates hundreds of phosphodiesterase enzymes and each enzyme can enzymatically cleave several cGMP molecules. This amplification cascade, therefore, produces a very large chemical signal from a single photon [74]. Another example of biochemical amplified activation of an ion channel is the phosphoinositide cascade [73,75]. In this case, an extracellular signal, such as a hormone, is recognized at the cell membrane and triggers the activation of the enzyme phospholipase C located at the membrane cytosolic leaflet. This enzyme produces the intracellular messenger IP3, which then diffuses through the cytoplasm and binds to Ca^{2+} ion channels in the endoplasmic reticulum membrane. The activated ion channel finally delivers Ca^{2+} ions into the cytosol, activating other biological processes. Each step of the cascade amplifies the original signal, resulting in an extremely large number of Ca^{2+} ions released per initial hormone molecule.

The applications of synthetic channels will unlikely require to mimic the extreme complexity of biological networks, but these networks can inspire new and improved strategies for sensing, drug delivery, and energy conversion. For instance, in the last years, researchers have developed synthetic systems that use enzymatic or electrochemical signal amplification to greatly improve the detection limits of nanochannel sensors.

Lin et al. presented a glucose-sensing channel based on an enzymatic cascade, see Fig. 2A.i [11]. The system consists of a symmetrical hour-glass single nanochannel etched in a polyimide membrane. The inner surface of this type of channels contains an excess of carboxylate groups generated during the etching procedure [66]. Part of these groups was used to covalently bind the enzymes glucose oxidase (GOx) and horseradish peroxidase (HRP) using carbodiimide chemistry. The remaining carboxylates confer a negative charge density to the inner surface of the channel at the operating pH (7.0). This negative charge requires compensation from mobile counter-cations, which increase the conductance of the channel [66]. Addition of glucose to the system results in its oxidation to gluconic acid by GOx. In parallel, GOx reduces dissolved oxygen to H_2O_2, which is subsequently dismuted by HRP to molecular oxygen and water. The gluconic acid generated in the process decreases the local pH within the pore and, therefore, neutralizes the surface-bound carboxylates. This process decreases the concentration of cations in the channel and lowers its conductance, see Fig. 2A.ii. The glucose sensor can function even in the absence of HRP, but the sensing efficiency is maximized in the presence of this enzyme because it eliminates H_2O_2, which is known to inhibit GOx [78]. The sensor responds to D-glucose concentrations in the micromolar range and shows almost no interference from other monosaccharides. Hou et al. reported a similar nano-device comprising a single conical nanochannel whose inner surface is modified by GOx [12]. Conical nanochannels are asymmetric with respect to the plane of the membrane, which confers them ion-current-rectifying capabilities [36]. The surface charge of the channel reported by Hou et al. is negative in the absence of glucose because of the presence of carboxylate groups. However, the addition of glucose results in a local decrease of pH due to the enzymatic production of gluconic acid. The drop in pH renders the surface charge of the channel positive because of the protonation of the basic residues of the immobilized GOx molecules. This charge inversion results in an inversion in the direction of rectification, which is the observable response of the sensor. The detection limit of the device is 1 nM, one of the lowest values reported for nanochannel glucose sensors. This very low detection limit supports the idea that dynamic signal amplification can be used to greatly enhance the sensing performance of nanochannel devices.

Fig. 2B.i shows another example of enzymatic amplification in a nanochannel that senses H_2O_2 reported by Ali et al. [76]. In this case, the inner surface of a single conical nanochannel is modified by covalently bound HRP. The channel senses H_2O_2 in the presence of ABTS. Under these conditions, the enzyme catalyzes the reduction of H_2O_2 to water and oxidizes ABTS to its radical cation, $ABTS^{\bullet+}$. This enzymatic reaction decreases the current of the nanochannel (see Fig. 2B.ii) and introduces large current fluctuations. Note that the channel is always cation-selective because of the presence of surface carboxylates. The authors ascribed the decrease in channel conductance to the fact that $ABTS^{\bullet+}$ may replace K^+ ions (which originated in the KCl electrolyte) as the main counter-ion compensating the charge of the carboxylates within the channel. This process reduces the conductance because $ABTS^{\bullet+}$ is bulkier and less mobile than K^+ and because electrostatic binding of $ABTS^{\bullet+}$ to the carboxylates may immobilize these ions. Once again, the chemical amplification mechanism allows reaching a very small detection limit for H_2O_2 (nanomolar range).

Pérez-Mitta et al. reported a nanofluidic diode for sensing urea, which uses enzymatic signal amplification to revert the polarity of the diode, see Fig. 2C.i [53]. In this example, the inner surface of a track-etched asymmetrically shaped nanochannel was modified with a layer of poly(allyl amine), PAH, a weak cationic polyelectrolyte. The adsorption of PAH occurs via the electrostatic interaction of the positively charged ammonium groups in the polymer and the negatively charged carboxylates on the inner surface of the channel. The negatively charged enzyme urease was then electrostatically adsorbed onto the PAH layer. The net charge

drug delivery, and energy conversion. For instance, in the last years, researchers have developed synthetic systems that use enzymatic or electrochemical signal amplification to greatly improve the detection limits of nanochannel sensors.

Lin et al. presented a glucose sensing channel based on an

the diode, see Fig. 2C.i [53]. In this example, the inner surface of a track-etched asymmetrically shaped nanochannel was modified with a layer of poly(allyl amine), PAH, a weak cationic polyelectrolyte. The adsorption of PAH occurs via the electrostatic interaction of the positively charged ammonium groups in the

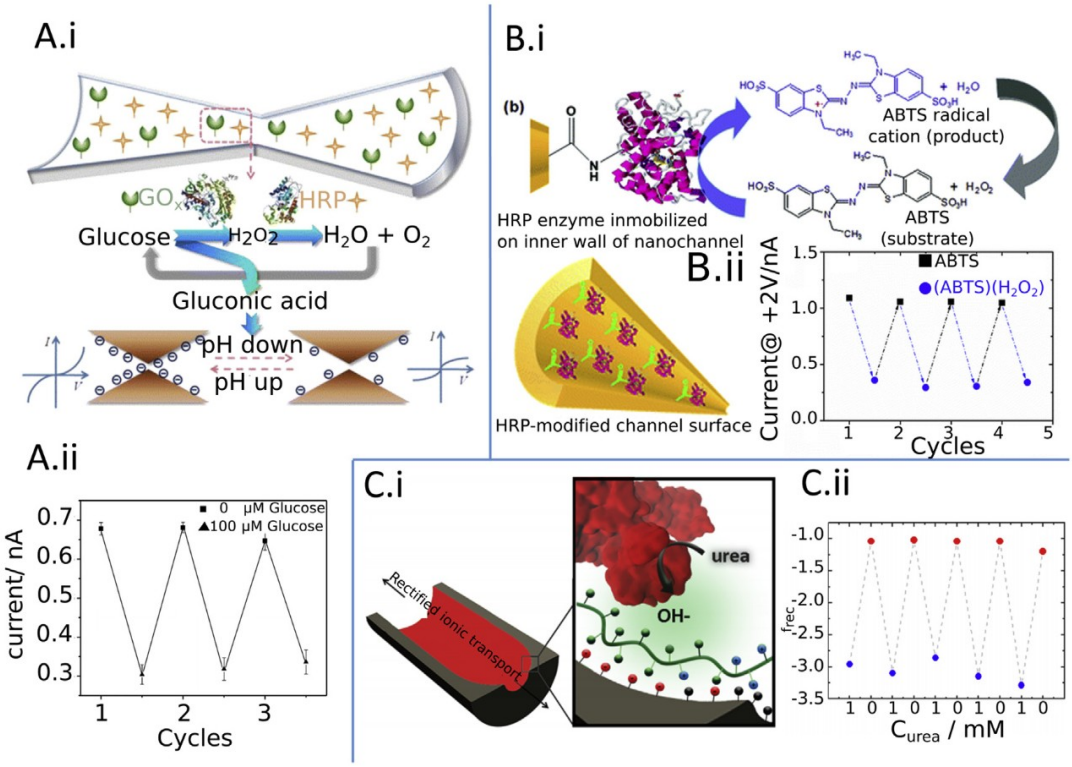

Fig. 2. Examples of signal amplification strategies for nanochannel sensing. A.i) An hourglass nanochannel is modified by glucose oxidize (GOx) and horseradish peroxidase (HRP). In the presence of glucose, the enzymatic reactions trigger a decrease of the pH within the channel, which protonates surface-bound carboxylate groups and, therefore, decreases the net surface charge of the channel and lowers its conductance (see effect of glucose on current in panel A.ii). Reproduced and adapted with permission from Ref. [11]. Copyright 2014 American Chemical Society. B.i) The inner surface of a conical nanochannel is modified by horseradish peroxidase. In the presence of H_2O_2 and ABTS, the channel conductance decreases because of the formation of $ABTS^{\bullet+}$ (see effect of H_2O_2 on current in panel B.ii). Reproduced and adapted with permission from Ref. [76]. Copyright 2011 American Chemical Society C.i) An asymmetrically shaped nanochannel is modified with a layer of PAH (a weak polyelectrolyte) and a second layer of urease. Hydrolysis of urea by urease increases the inner pH within the channel, which shifts the surface charge from positive to negative and, therefore, reverts the direction of current rectification (see effect of urea of current rectification ratio in panel C.ii). Reproduced and adapted with permission from Ref. [77]. Copyright 2018 American Chemical Society.

of the assembly was positive because of an excess of ammonium groups from PAH, thus the channel behaves as an anion conductor and exhibits rectifying diode-like properties. Addition of urea to the system results in its hydrolysis by urease, a reaction that produces hydroxyl ions and increases the local pH inside the channel. This basification reaction neutralizes the ammonium groups of PAH, ultimately leading to an inversion of the surface charge of the channel, which becomes dominated by the negative charges of the carboxylates. The inversion of the surface charge results in an inversion in the direction of current rectification (Fig. 2C.ii). This signal is very sensitive to the concentration of urea in solution and the limit of detection (1 nM of urea) is the lowest reported for an enzymatic-based urea sensor.

There exist examples of enzyme-amplified chemical signals where the enzymatic reaction changes the inner composition of the channel in the presence of the analyte. For example, HRP in the presence of H_2O_2 has been used to grow a polymer inside a nanochannel [79]. This polymer blocks the ion current through the channel, generating a resistive signal. In another example of enzyme-based amplification, a Cu^{2+}-activated DNAzyme was grafted to the inner surface of a conical nanochannel [80]. This system has high cation conductivity because of the presence of negative charges from DNA strands. Upon addition of Cu^{2+} at concentrations as low as 10 nM, the DNA is cleaved and the cation current through the channel decreases. In another study by Majumdar and coworkers, a nanochannel modified by poly(L-lysine) senses the concentration of the enzyme trypsin in solution. This enzyme diffuses into the channel, hydrolyzing the poly(L-lysine), which is a positively charged polyelectrolyte. The charges of poly(L-lysine) are originally compensating the intrinsic negative charges on the nanochannel walls and, therefore, upon digestion of the polyelectrolyte, the net surface charge of the channel increases. This mechanism results in an increase in conductance, which depends on the concentration of trypsin in solution.

Signal amplification can be achieved without enzymes using electrochemical methods. Fig. 3A shows a nanopore incorporating two independently addressable electrodes in its structure [81,82]. An electrochemically active analyte can be sensed in this system by oxidizing it in one electrode and reducing it in the other. The very small volume of the nanochannel results in a very large number of redox cycles before the analyte can diffuse away from the pore. These redox cycles result in a large amplification of the current response of the device. Bipolar electrochemistry is another interesting way to control transport in nanochannels, which avoids the need of wiring multiple independently addressable electrodes [33]. Fig. 3B shows an example of signal amplification based on the combination of a nanochannel and a bipolar electrode, which was applied to intracellular NADH sensing [83]. The interior of a glass nanopipette was coated with a thin layer of gold that was then modified with a self-assembled monolayer of catechol-terminated thiols. Applying a *trans*-pipette voltage induces a bipolar electric potential across the gold layer, which oxidizes the catechol far from the tip and reduces H^+ to H_2 near the tip (see left panel in Fig. 3B).

enzyme-based amplification, a Cu^{2+}-activated DNAzyme was grafted to the inner surface of a conical nanochannel [80]. This system has high cation conductivity because of the presence of negative charges from DNA strands. Upon addition of Cu^{2+} at concentrations as low as 10 nM, the DNA is cleaved and the cation

Fig. 3B shows an example of signal amplification based on the combination of a nanochannel and a bipolar electrode, which was applied to intracellular NADH sensing [83]. The interior of a glass nanopipette was coated with a thin layer of gold that was then modified with a self-assembled monolayer of catechol-terminated

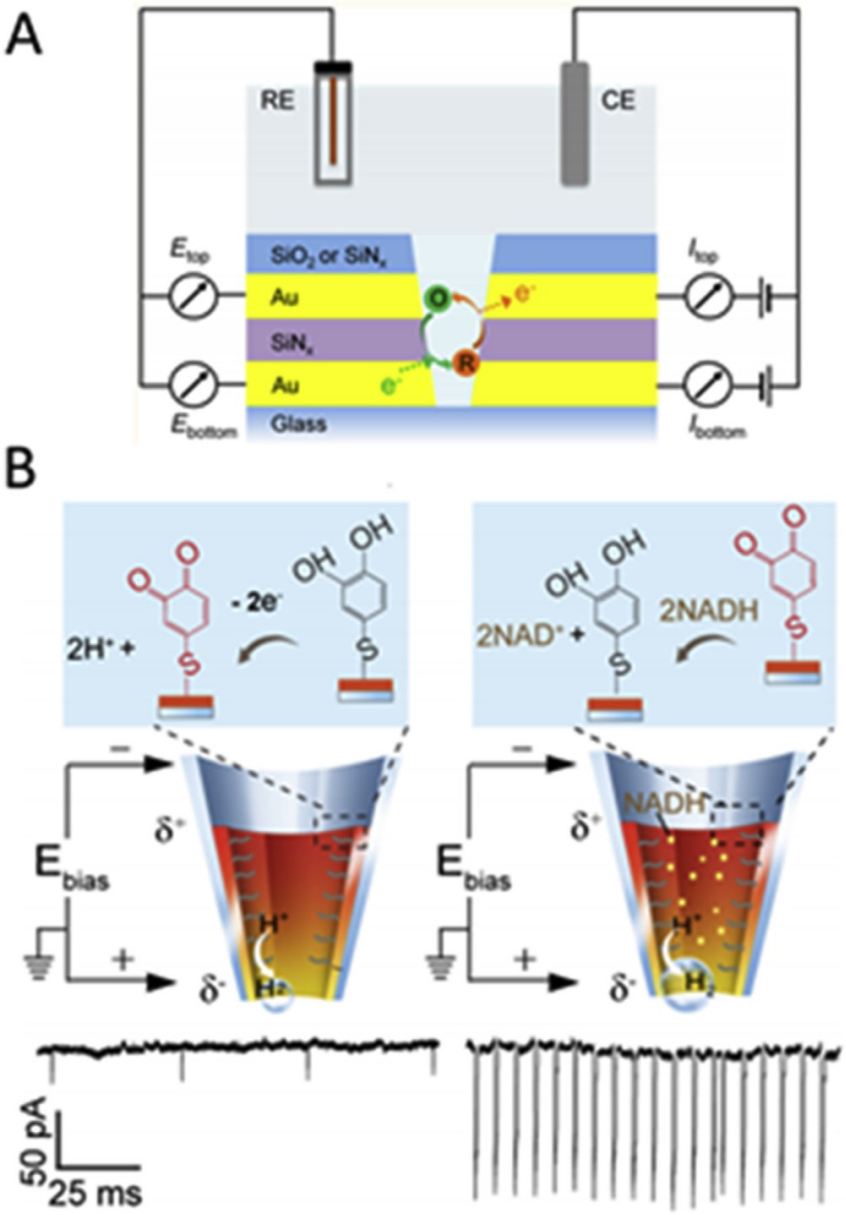

Fig. 3. A. Signal amplification in a nanopore by redox recycling. Because of the nanoconfinement effect of the pore, a redox-active analyte undergoes several oxidation/reduction cycles by two independently addressable electrodes, which results in a large enhancement in the electrical current. Reproduced and adapted from Ref. [81]. Copyright 2016 American Chemical Society. B. Signal amplification by bubble formation in a gold coated nanopipette. NADH oxidation (catalyzed by catechol) far from the pipette tip injects electrons into the Au layer. These electrons reduce H^+ to H_2 at the tip. The H_2 bubble blocks ion currents through the pipette and then dissolves, producing resistive pulses (bottom panels). Reproduced and adapted from Ref. [83]. Copyright 2018 American Chemical Society.

NADH in solution reduces the oxidized catechol, recycling it. This process leads to a fast build-up of a H_2 bubble in the tip. This bubble transiently blocks the ion current through the pipette before dissolving, which leads to a resistive pulse (see lower panels in Fig. 3B). Therefore, in this mechanism, a large change in conductance is produced by the reaction of a very small number of NADH molecules, greatly amplifying its chemical signal and enabling the measurement of NADH in living cells.

4. Transport of large cargoes

A major area in nanofluidics is the selective manipulation of fluxes of biomolecules and nanoobjects. The best known and most studied example is by far that of DNA translocation through nanopores because of its outstanding importance for genome sequencing. In this example, the partial blockage of the ionic current (resistive pulse) measured during the translocation of a single DNA molecule is used to infer the sequence of DNA bases [84–86]. Nanopore-based DNA-sequencing is now a commercially available technology [87] and a lot of effort is still being invested to improve this technology and to develop sensing devices for other biomolecules or particles [88–91].

Despite the impressive advances in the development of nanopore-based sensing devices, these systems usually exhibit low selectivity in the translocation of cargo and poor gating capabilities. In other words, it remains challenging to selectively filter one type

tance is produced by the reaction of a very small number of NADH molecules, greatly amplifying its chemical signal and enabling the measurement of NADH in living cells.

Nanopore-based DNA-sequencing is now a commercially available technology [87] and a lot of effort is still being invested to improve this technology and to develop sensing devices for other biomolecules or particles [88–91].

Despite the impressive advances in the development of

of biomolecule from a mixture and to externally control the permeability of the channel. Transport selectivity is achieved in nature by the nuclear pore complex (NPC), which is an impressive protein structure anchored in the nuclear envelope that transports biomolecules between the cytoplasm and the nucleus. It is permeable to small molecules such as water and ions, but cargoes larger than 40 kDa need to be recognized by specific transport receptors to translocate through the pore [92]. The selectivity filter of the NPC is constituted by several intrinsically disordered proteins, the FG-Nups, that are end-tethered to the NPC framework and extend into the channel to interact with the cargo. One important conclusion that emerges from the study of this biological system is the multifactorial nature of transport selectivity, which depends on the presence of different and complementary interactions between cargo and nanopore [93,94], the size of the channel, and changes in molecular organization inside the pores triggered by the presence of the cargoes and/or other macromolecules [95]. A complete understanding of the transport mechanisms operating in the NPC is still missing, but such fundamental understanding can unlock synthetic nanopores with unprecedented transport selectivity. Theoretical tools have been used to shed some light on the transport properties of both the NPC and synthetic NPC-inspired polymer-brush-modified nanopores. These studies have revealed the existence of a synergistic combination of different interactions in the translocation of cargoes through the NPC and their synthetic analogs. The barrier for translocation decreases when the cargo has a charge of opposite sign to that of the brush. It also decreases when both the cargo and the brush are hydrophobic. However, making the particle oppositely charged to brush and hydrophobic at the same time decreases the translocation barrier more than what one would expect from the sum of the individual contributions [93]. This synergistic non-additive effect may have further implications on the selectivity mechanisms of the NPC.

Artificial nanopores modified by polymer and protein brushes are promising systems for selective transporters that are inspired by the structure of the NPC, which can be used to better comprehend this fascinating biological nanostructure [96,97]. As an example, Emilson et al. fabricated nanopores modified with a poly(ethylene glycol) (PEG) brush, where the translocation of proteins can be turned on and off by the reversible binding of a single IgG antibody to the PEG chains [98]. Recent research works, aimed to understand the biophysics of the NPC, studied solid-state nanopores [99] and DNA-origami nanorings [100] modified by grafted FG-Nup chains. In one of these works, Ananth et al. [99] studied nanopores of different radii modified by the FG-Nup Nsp1 and a Nsp1 mutant in which some hydrophobic amino acids (phenylalanine, isoleucine, leucine, and valine) were replaced by the hydrophilic amino acid serine. Based on conductance measurements and molecular dynamic simulations, the authors concluded that the protein plug inside the pore modified by the mutated protein was less compact than that of the pore reconstructed using the native FG-Nups. Interestingly, the pore modified by the native FG-Nups transported the nuclear transport receptor (NTR) Kap95 with a much higher translocation frequency than a non-NTR protein of similar size (tCherry). On the other hand, the pore modified by the mutated protein did not exhibit such selectivity. Coarse-grained molecular dynamic simulations suggested that the selectivity for Kap95 observed for the nanopore modified with native FG-Nups arises from the compensation of steric repulsions and hydrophobic attractions between the FG-Nups and Kap95, which decreases the free-energy barrier for translocation [99].

Theoretical calculations can provide design principles for stimuli-gated transport in polymer-modified nanochannels and nanopores. For example, Lopez et al. modeled the behavior of nanochannels functionalized with poly(acrylic acid) brushes and their interaction with calcium cations using a molecular theory. This work proposed that calcium ions could induce the collapse of the polymer brush, gating the transport of cargoes through the pore. Huang et al. [101] theoretically designed pH-switchable nanopores using end-graft amphiphilic diblock copolymers on their inner surface. Their prediction is that in this system, pH can be used to tune the selective transport of cargoes with different surface hydrophobicity and charge. The full free energy landscape of a nanoparticle interacting with a polymer-brush-modified nanopore was studied in a recent publication [102]. This analysis allowed predicting the possible translocation routes for the particle through the nanopore. Fig. 4A shows a schematic representation of the pore modified by a polymer brush. Fig. 4B i,ii, iii shows color maps of the free energy of the nanoparticle-pore system, where the blue regions represent positions where the particle has a larger free energy than in the bulk and red regions indicate zones where the free energy is smaller than in the bulk. The black line shows the translocation route (determined as the minimum free energy pathway). Interestingly, increasing the absolute value of the particle-polymer attractive energy (ε_{ps}) shifts the translocation route from the central axis of the pore toward its wall. A similar effect was observed when decreasing the size of the particle. To study the permeability of the pore for a given cargo, it is useful to analyze the free energy of the system along the translocation pathway, see Fig. 4B.iv. An almost flat energy profile (black curve) ensures the fastest translocation of the particles through the pore [103]. If the profile has a barrier (red curve), then translocation will be slowed down compared to the previous case and it can even become infeasible if the barrier height is much larger than the thermal energy (k_BT). Finally, in the case where the energy profile has a well (blue curve), then the particle can get trapped inside the pore. This example shows that, by careful manipulation of the polymer–particle interaction, one can in principle optimize the rate of translocation for a given type of particle.

5. Conclusions and outlook

By many metrics, the performance of nanopores and nanochannels had improved at an accelerated rate in the last five years. Important transport mechanisms and behaviors, such as current rectification, unipolar transport, polymer translocation through pores, and ion-gating mechanisms, are now relatively well understood from a fundamental point of view and well demonstrated by many practical examples. Many of these phenomena have important practical applications: polymer translocation holds the potential of enabling DNA-sequencing nanopores and current rectification and gating are crucial mechanisms for the development of nanochannel sensors. As these research areas and applications ripe, there are many other fundamental challenges that need to be addressed to unlock the full potential of these nanodevices. We have reviewed here recent work in what we believe are three of these key challenges: i) selective ion transport, ii) integration of nanopores and nanochannels with chemical networks, and iii) gating and selectivity in the transport of macromolecules and nanoobjects. In all three cases, we provided a brief analysis of related biological mechanisms, which we hope will serve as a source of bioinspiration.

Charge selectivity (i.e., transport of anions vs cations) is nowadays a very well-known phenomenon in solid-state nanochannels and nanopores. Such selectivity is generally introduced by the presence of charged groups on the inner walls of the channel, which results in an enhancement of the concentration of the oppositely charged ions. These counterions are, therefore, selectively transported through the channel in a phenomenon known as

that the selectivity for Kap95 observed for the nanopore modified with native FG-Nups arises from the compensation of steric repulsions and hydrophobic attractions between the FG-Nups and Kap95, which decreases the free-energy barrier for translocation [99].

Charge selectivity (i.e., transport of anions vs cations) is nowadays a very well-known phenomenon in solid-state nanochannels and nanopores. Such selectivity is generally introduced by the presence of charged groups on the inner walls of the channel

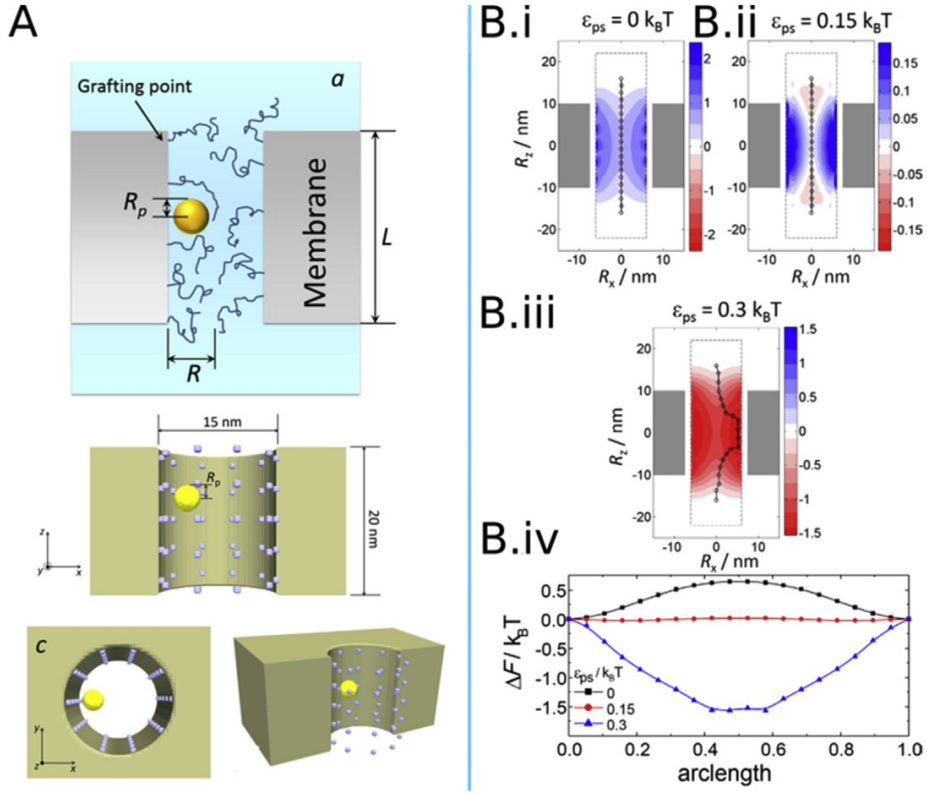

Fig. 4. A) Schematic representation of system studied in Ref. [102]. The nanoparticle is shown in yellow and the blue circles indicate the position of the grafting points of the polymer. B.i,ii,iii) Color map of the free energy (in k_BT) of a nanoparticle inside the polymer-brush-modified nanopore as a function of its position in the x (R_x) and z (R_z) directions (see coordinate system in panel A) for $R_y = 0$ (the channel axis is located at $R_x = 0$ and $R_y = 0$) for different particle–segment interaction strengths. The black points indicate the minimum free-energy pathway for the translocation of nanoparticles through the nanopore. B.iv) Free energy along the minimum free-energy pathway. Reproduced and adapted from Ref. [102]. Copyright 2018 IOP Publishing Ltd.

unipolar transport [104]. However, recent works have claimed transport selectivity between ions of the same charge. In these examples, selectivity is generally achieved by using sub-nanometer channels that filter hydrated ions by size and/or by stripping hydration waters. These mechanisms share many similarities with transport in biological ion channels. It is interesting to note that while the reports reviewed here are experimental examples, many of them include results from atomistic molecular dynamic simulations. This observation stresses the importance of theory to gain a molecular insight of the mechanisms that enable transport selectivity.

Some synthetic devices have recently started to use strategies that were exclusive of biological channels and pores, such as reactive signal amplification. In this case, the goal is to use cascades of chemical reactions to amplify a very small chemical signal into a measurable current. The examples in the literature are truly promising but their number is still scarce and their complexity is significantly lower than that of natural signaling pathways. Interestingly, although there are a few examples of enzymatic and electrochemical amplification, other strategies found in biological networks (such as feedback loops) seem to be unexplored in synthetic pores and channels. The theoretical description of chemical reactive amplification systems has lag behind the seminal experimental work in the field. Modeling has much to offer to our fundamental understanding of these systems, although it is also a challenging task because of the coexistence of strikingly different physical and chemical phenomena in these systems, which include ion and solvent fluxes, enzymatic chemical reactions, and soft matter physics.

Translocation of macromolecules and nanoobjects through bare nanochannels is well documented. However, gated and/or selective transport of objects substantially larger than simple ions is still difficult to achieve. Inspired by the transport mechanisms of the nuclear pore complex, we and others have theoretically proposed and designed nanopores whose inner walls are coated by polymer or polyelectrolyte brushes. These brushes interact with potential cargoes and generate selectivity by balancing attractive and repulsive interactions. This balance can be achieved, for example, by tuning the charge of the grafted polyelectrolyte using pH or by controlling hydrophobic interactions by the choice of the type of polymer or the particle surface chemistry. There are only a few experimental examples of transport of proteins through polymer-brush modified nanopores, which shows that this research direction is challenging but also full of interesting opportunities.

Recent achievements in nanofluidics are at the same time numerous, practically relevant, and highly creative. The field is quickly evolving to satisfy technological demands in very diverse areas, including biosensing, energy conversion, and chemical separation. The scientific and technological challenges reviewed here are critical to the success of these applications and, for this reason, we expect to see great advances in these directions in the near future. For example, the separation of ions of the same charge and similar size and chemical properties may enable the recovery and separation of heavy metals, a process of upmost economic and environmental relevance. It can also convey novel cheap and environmentally friendly methods to purify and obtain lithium salts from brines and (ideally) seawater, which has become a pressing need because of the importance of this element in

reactive amplification systems has lag behind the seminal experimental work in the field. Modeling has much to offer to our fundamental understanding of these systems, although it is also a challenging task because of the coexistence of strikingly different future. For example, the separation of ions of the same charge and similar size and chemical properties may enable the recovery and separation of heavy metals, a process of upmost economic and environmental relevance. It can also convey novel cheap and

batteries for mobile electronics and the automotive industry. On the other hand, the integration of nanopores and nanochannels into chemical networks and the capability of transporting cargoes larger than single ions are crucial technologies that hold the key for the fabrication of integrated nanochannel systems. A fascinating prospect is that of iontronic networks integrated in a single chip. These sophisticated nanofluidic devices may one day combine coupled biochemical reactions, supramolecular chemical recognition, and nanoscale materials to simultaneously sense a spectrum of chemical and physical variables, provide a readable output signal, and ultimately deliver small molecules, macromolecules, and/or nanoparticles in response.

In summary, we have reviewed three interesting topics that pose fundamental and current challenges in nanopore and nanochannel science. We expect to see great advances in these research directions in forthcoming years, powered by innovative fabrication and modification methods, guided by new fundamental insights provided from theory and computer simulations and inspired by the ever-surprising transport mechanisms evolved in living organisms.

Declaration of competing interest

The authors declare that they have no known competing financial interests or personal relationships that could have appeared to influence the work reported in this paper.

Acknowledgments

IS acknowledges support from NSF, Div. of Chem. Bioeng. Env. and Transp. Sys. 1833214. MT is a fellow of CONICET and acknowledges support from ANPCyT (PICT 2015 0099 and PICT 2016 0154) and University of Buenos Aires (UBACyT 20020170200215BA).

References

[1] M. Tagliazucchi, I. Szleifer, Transport mechanisms in nanopores and nanochannels: can we mimic nature? Mater. Today 18 (2015) 131–142.
[2] X. Hou, W. Guo, F. Xia, F.-Q. Nie, H. Dong, Y. Tian, L. Wen, L. Wang, L. Cao, Y. Yang, A biomimetic potassium responsive nanochannel: G-quadruplex DNA conformational switching in a synthetic nanopore, J. Am. Chem. Soc. 131 (2009) 7800–7805.
[3] Z.S. Siwy, M.R. Powell, A. Petrov, E. Kalman, C. Trautmann, R.S. Eisenberg, Calcium-induced voltage gating in single conical nanopores, Nano Lett. 6 (2006) 1729–1734.
[4] Q. Liu, K. Xiao, L. Wen, H. Lu, Y. Liu, X.-Y. Kong, G. Xie, Z. Zhang, Z. Bo, L. Jiang, Engineered ionic gates for ion conduction based on sodium and potassium activated nanochannels, J. Am. Chem. Soc. 137 (2015) 11976–11983, https://doi.org/10.1021/jacs.5b04911.
[5] G. Pérez-Mitta, A.G. Albesa, W. Knoll, C. Trautmann, M.E. Toimil-Molares, O. Azzaroni, Host–guest supramolecular chemistry in solid-state nanopores: potassium-driven modulation of ionic transport in nanofluidic diodes, Nanoscale 7 (2015) 15594–15598.
[6] Y. Tian, Z. Zhang, L. Wen, J. Ma, Y. Zhang, W. Liu, J. Zhai, L. Jiang, A biomimetic mercury (II)-gated single nanochannel, Chem. Commun. 49 (2013) 10679–10681.
[7] Y. Shang, Y. Zhang, P. Li, J. Lai, X.-Y. Kong, W. Liu, K. Xiao, G. Xie, Y. Tian, L. Wen, DNAzyme tunable lead (II) gating based on ion-track etched conical nanochannels, Chem. Commun. 51 (2015) 5979–5981.
[8] L. Gao, P. Li, Y. Zhang, K. Xiao, J. Ma, G. Xie, G. Hou, Z. Zhang, L. Wen, L. Jiang, A bio-inspired, sensitive, and selective ionic gate driven by silver (I) ions, Small 11 (2015) 543–547, https://doi.org/10.1002/smll.201400658.
[9] Q. Liu, K. Xiao, L. Wen, Y. Dong, G. Xie, Z. Zhang, Z. Bo, L. Jiang, A fluoride-driven ionic gate based on a 4-aminophenylboronic acid-functionalized asymmetric single nanochannel, ACS Nano 8 (2014) 12292–12299.
[10] G. Xie, K. Xiao, Z. Zhang, X. Kong, Q. Liu, P. Li, L. Wen, L. Jiang, A bioinspired switchable and tunable carbonate-activated nanofluidic diode based on a single nanochannel, Angew. Chem. Int. Ed. 54 (2015) 13664–13668.
[11] L. Lin, J. Yan, J. Li, Small-molecule triggered cascade enzymatic catalysis in hour-glass shaped nanochannel reactor for glucose monitoring, Anal. Chem. 86 (2014) 10546–10551, https://doi.org/10.1021/ac501983a.
[12] G. Hou, H. Zhang, G. Xie, K. Xiao, L. Wen, S. Li, Y. Tian, L. Jiang, Ultratrace detection of glucose with enzyme-functionalized single nanochannels, J. Mater. Chem. A. 2 (2014) 19131–19135.
[13] S.M. Iqbal, D. Akin, R. Bashir, Solid-state nanopore channels with DNA selectivity, Nat. Nanotechnol. 2 (2007) 243.
[14] N. Liu, Y. Jiang, Y. Zhou, F. Xia, W. Guo, L. Jiang, Two-way nanopore sensing of sequence-specific oligonucleotides and small-molecule targets in complex matrices using integrated DNA supersandwich structures, Angew. Chem. Int. Ed. 52 (2013) 2007–2011.
[15] Z. Sun, F. Zhang, X. Zhang, D. Tian, L. Jiang, H. Li, Chiral recognition of Arg based on label-free PET nanochannel, Chem. Commun. 51 (2015) 4823–4826.
[16] G. Xie, W. Tian, L. Wen, K. Xiao, Z. Zhang, Q. Liu, G. Hou, P. Li, Y. Tian, L. Jiang, Chiral recognition of L-tryptophan with beta-cyclodextrin-modified biomimetic single nanochannel, Chem. Commun. 51 (2015) 3135–3138.
[17] Y. Xu, X. Sui, S. Guan, J. Zhai, L. Gao, Olfactory sensory neuron-mimetic CO2 activated nanofluidic diode with fast response rate, Adv. Mater. Deerfield Beach Fla. 27 (2015) 1851.
[18] Y. Xu, X. Sui, J. Jiang, J. Zhai, L. Gao, Smooth muscle cell-mimetic CO-regulated ion nanochannels, Adv. Mater. 28 (2016) 10780–10785.
[19] M. Ali, B. Yameen, R. Neumann, W. Ensinger, W. Knoll, O. Azzaroni, Biosensing and supramolecular bioconjugation in single conical polymer nanochannels. Facile incorporation of biorecognition elements into nanoconfined geometries, J. Am. Chem. Soc. 130 (2008) 16351–16357, https://doi.org/10.1021/ja8071258.
[20] B. Yameen, M. Ali, R. Neumann, W. Ensinger, W. Knoll, O. Azzaroni, Single conical nanopores displaying pH-tunable rectifying characteristics. Manipulating ionic transport with zwitterionic polymer brushes, J. Am. Chem. Soc. 131 (2009) 2070–2071.
[21] B. Yameen, M. Ali, R. Neumann, W. Ensinger, W. Knoll, O. Azzaroni, Synthetic proton-gated ion channels via single solid-state nanochannels modified with responsive polymer brushes, Nano Lett. 9 (2009) 2788–2793, https://doi.org/10.1021/nl901403u.
[22] M. Tagliazucchi, O. Azzaroni, I. Szleifer, Responsive polymers end-tethered in solid-state nanochannels: when nanoconfinement really matters, J. Am. Chem. Soc. 132 (2010) 12404–12411.
[23] A. Andrieu-Brunsen, S. Micoureau, M. Tagliazucchi, I. Szleifer, O. Azzaroni, G.J. Soler-Illia, Mesoporous hybrid thin film membranes with PMETAC@ silica architectures: controlling ionic gating through the tuning of polyelectrolyte density, Chem. Mater. 27 (2015) 808–821.
[24] M. Lepoitevin, G. Nguyen, M. Bechelany, E. Balanzat, J.-M. Janot, S. Balme, Combining a sensor and a pH-gated nanopore based on an avidin–biotin system, Chem. Commun. 51 (2015) 5994–5997, https://doi.org/10.1039/C4CC10087E.
[25] G.-C. Liu, M.-J. Gao, W. Chen, X.-Y. Hu, L.-B. Song, B. Liu, Y.-D. Zhao, pH-modulated ion-current rectification in a cysteine-functionalized glass nanopipette, Electrochem, Commun. Now. 97 (2018) 6–10, https://doi.org/10.1016/j.elecom.2018.09.017.
[26] K. Xiao, G. Xie, P. Li, Q. Liu, G. Hou, Z. Zhang, J. Ma, Y. Tian, L. Wen, L. Jiang, A biomimetic multi-stimuli-response ionic gate using a hydroxypyrene derivation-functionalized asymmetric single nanochannel, Adv. Mater. 26 (2014) 6560–6565.
[27] G. Wang, A.K. Bohaty, I. Zharov, H.S. White, Photon gated transport at the glass nanopore electrode, J. Am. Chem. Soc. 128 (2006) 13553–13558.
[28] T. Ma, M. Walko, M. Lepoitevin, J.-M. Janot, E. Balanzat, A. Kocer, S. Balme, Combining light-gated and pH-responsive nanopore based on PEG-spiropyran functionalization, Adv. Mater. Interfaces 5 (2018) 1701051, https://doi.org/10.1002/admi.201701051.
[29] M. Zhang, X. Hou, J. Wang, Y. Tian, X. Fan, J. Zhai, L. Jiang, Light and pH cooperative nanofluidic diode using a spiropyran-functionalized single nanochannel, Adv. Mater. 24 (2012) 2424–2428, https://doi.org/10.1002/adma.201104536.
[30] W.-J. Lan, D.A. Holden, H.S. White, Pressure-dependent ion current rectification in conical-shaped glass nanopores, J. Am. Chem. Soc. 133 (2011) 13300–13303.
[31] B. Yameen, M. Ali, R. Neumann, W. Ensinger, W. Knoll, O. Azzaroni, Ionic transport through single solid-state nanopores controlled with thermally nanoactuated macromolecular gates, Small 5 (2009) 1287–1291.
[32] Y. Zhou, W. Guo, J. Cheng, Y. Liu, J. Li, L. Jiang, High-temperature gating of solid-state nanopores with thermo-responsive macromolecular nanoactuators in ionic liquids, Adv. Mater. 24 (2012) 962–967.
[33] M. Tagliazucchi, I. Szleifer, Salt pumping by voltage-gated nanochannels, J. Phys. Chem. Lett. 6 (2015) 3534–3539.
[34] W. Guan, R. Fan, M.A. Reed, Field-effect reconfigurable nanofluidic ionic diodes, Nat. Commun. 2 (2011) 506.
[35] J. Cervera, B. Schiedt, P. Ramirez, A Poisson/Nernst-Planck model for ionic transport through synthetic conical nanopores, EPL Europhys. Lett. 71 (2005) 35.
[36] Z.S. Siwy, Ion-current rectification in nanopores and nanotubes with broken symmetry, Adv. Funct. Mater. 16 (2006) 735–746.
[37] Z. Siwy, A. Fuliński, Fabrication of a synthetic nanopore ion pump, Phys. Rev. Lett. 89 (2002) 198103.
[38] H. Daiguji, Y. Oka, K. Shirono, Nanofluidic diode and bipolar transistor, Nano Lett. 5 (2005) 2274–2280.

Small 11 (2015) 543–547, https://doi.org/10.1002/smll.201400658.
[9] Q. Liu, K. Xiao, L. Wen, Y. Dong, G. Xie, Z. Zhang, Z. Bo, L. Jiang, A fluoride-driven ionic gate based on a 4-aminophenylboronic acid-functionalized asymmetric single nanochannel, ACS Nano 8 (2014) 12292–12299.
[10] G. Xie, K. Xiao, Z. Zhang, X. Kong, Q. Liu, P. Li, L. Wen, L. Jiang, A bioinspired switchable and tunable carbonate-activated nanofluidic diode based on a
[35] J. Cervera, B. Schiedt, P. Ramirez, A Poisson/Nernst-Planck model for ionic transport through synthetic conical nanopores, EPL Europhys. Lett. 71 (2005) 35.
[36] Z.S. Siwy, Ion-current rectification in nanopores and nanotubes with broken symmetry, Adv. Funct. Mater. 16 (2006) 735–746.
[37] Z. Siwy, A. Fuliński, Fabrication of a synthetic nanopore ion pump, Phys. Rev.

[39] I. Vlassiouk, S. Smirnov, Z. Siwy, Nanofluidic ionic diodes. Comparison of analytical and numerical solutions, ACS Nano 2 (2008) 1589–1602.
[40] I. Vlassiouk, Z.S. Siwy, Nanofluidic diode, Nano Lett. 7 (2007) 552–556.
[41] M. Tagliazucchi, Y. Rabin, I. Szleifer, Transport rectification in nanopores with outer membranes modified with surface charges and polyelectrolytes, ACS Nano 7 (2013) 9085–9097, https://doi.org/10.1021/nn403686s.
[42] A. Liu, M. Tang, J. Xi, L. Gao, Y. Zheng, H. Luo, X. Hu, F. Zhao, M. Reppel, J. Hescheler, Functional characterization of inward rectifier potassium ion channel in murine fetal ventricular cardiomyocytes, Cell. Physiol. Biochem. 26 (2010) 413–420.
[43] Z. Zhang, X.-Y. Kong, K. Xiao, Q. Liu, G. Xie, P. Li, J. Ma, Y. Tian, L. Wen, L. Jiang, Engineered asymmetric heterogeneous membrane: a concentration-gradient-driven energy harvesting device, J. Am. Chem. Soc. 137 (2015) 14765–14772, https://doi.org/10.1021/jacs.5b09918.
[44] Y. Zhao, J.-M. Janot, E. Balanzat, S. Balme, Mimicking pH-gated ionic channels by polyelectrolyte complex confinement inside a single nanopore, Langmuir 33 (2017) 3484–3490, https://doi.org/10.1021/acs.langmuir.7b00377.
[45] K. Xiao, L. Wen, L. Jiang, Biomimetic solid-state nanochannels: from fundamental research to practical applications, Small 12 (2016) 2810–2831.
[46] H. Zhang, Y. Tian, L. Jiang, Fundamental studies and practical applications of bio-inspired smart solid-state nanopores and nanochannels, Nano Today 11 (2016) 61–81, https://doi.org/10.1016/j.nantod.2015.11.001.
[47] M. Lepoitevin, T. Ma, M. Bechelany, J.-M. Janot, S. Balme, Functionalization of single solid state nanopores to mimic biological ion channels: a review, Adv. Colloid Interface Sci. 250 (2017) 195–213, https://doi.org/10.1016/j.cis.2017.09.001.
[48] R. Li, X. Fan, Z. Liu, J. Zhai, Smart bioinspired nanochannels and their applications in energy-conversion systems, Adv. Mater. 29 (2017) 1702983.
[49] Z. Long, S. Zhan, P. Gao, Y. Wang, X. Lou, F. Xia, Recent advances in solid nanopore/channel analysis, Anal. Chem. 90 (2017) 577–588.
[50] Z. Zhang, L. Wen, L. Jiang, Bioinspired smart asymmetric nanochannel membranes, Chem. Soc. Rev. 47 (2018) 322–356, https://doi.org/10.1039/C7CS00688H.
[51] Y. Zhu, K. Zhan, X. Hou, Interface design of nanochannels for energy utilization, ACS Nano 12 (2018) 908–911.
[52] D. Ding, P. Gao, Q. Ma, D. Wang, F. Xia, Biomolecule-functionalized solid-state ion nanochannels/nanopores: features and techniques, Small (2019) 1804878, https://doi.org/10.1002/smll.201804878.
[53] G. Pérez-Mitta, M.E. Toimil-Molares, C. Trautmann, W.A. Marmisollé, O. Azzaroni, Molecular design of solid-state nanopores: fundamental concepts and applications, Adv. Mater. (2019) 1901483, https://doi.org/10.1002/adma.201901483.
[54] Z. Zhu, D. Wang, Y. Tian, L. Jiang, Ion/molecule transportation in nanopores and nanochannels: from critical principles to diverse functions, J. Am. Chem. Soc. 141 (2019) 8658–8669, https://doi.org/10.1021/jacs.9b00086.
[55] F. Marchini, D. Rubi, M. del Pozo, F.J. Williams, E.J. Calvo, Surface chemistry and lithium-ion exchange in LiMn2O4 for the electrochemical selective extraction of LiCl from natural salt lake brines, J. Phys. Chem. C 120 (2016) 15875–15883.
[56] S.P. Surwade, S.N. Smirnov, I.V. Vlassiouk, R.R. Unocic, G.M. Veith, S. Dai, S.M. Mahurin, Water desalination using nanoporous single-layer graphene, Nat. Nanotechnol. 10 (2015) 459.
[57] K. Murata, K. Mitsuoka, T. Hirai, T. Walz, P. Agre, J.B. Heymann, A. Engel, Y. Fujiyoshi, Structural determinants of water permeation through aquaporin-1, Nature 407 (2000) 599–605, https://doi.org/10.1038/35036519.
[58] D.A. Doyle, J.M. Cabral, R.A. Pfuetzner, A. Kuo, J.M. Gulbis, S.L. Cohen, B.T. Chait, R. MacKinnon, The structure of the potassium channel: molecular basis of K+ conduction and selectivity, Science 280 (1998) 69–77, https://doi.org/10.1126/science.280.5360.69.
[59] C. Lim, T. Dudev, Potassium versus sodium selectivity in monovalent ion channel selectivity filters, in: A. Sigel, H. Sigel, R.K.O. Sigel (Eds.), Alkali Met. Ions Their Role Life, Springer International Publishing, Cham, 2016, pp. 325–347, https://doi.org/10.1007/978-3-319-21756-7_10.
[60] C. Song, B. Corry, Intrinsic ion selectivity of narrow hydrophobic pores, J. Phys. Chem. B 113 (2009) 7642–7649, https://doi.org/10.1021/jp810102u.
[61] R.C. Rollings, A.T. Kuan, J.A. Golovchenko, Ion selectivity of graphene nanopores, Nat. Commun. 7 (2016) 11408.
[62] Y. Guo, Y. Ying, Y. Mao, X. Peng, B. Chen, Polystyrene sulfonate threaded through a metal–organic framework membrane for fast and selective lithium-ion separation, Angew. Chem. Int. Ed. 55 (2016) 15120–15124.
[63] M. Wang, W. Shen, S. Ding, X. Wang, Z. Wang, Y. Wang, F. Liu, A coupled effect of dehydration and electrostatic interactions on selective ion transport through charged nanochannels, Nanoscale 10 (2018) 18821–18828, https://doi.org/10.1039/C8NR04962A.
[64] P. Wang, M. Wang, F. Liu, S. Ding, X. Wang, G. Du, J. Liu, P. Apel, P. Kluth, C. Trautmann, Ultrafast ion sieving using nanoporous polymeric membranes, Nat. Commun. 9 (2018) 569.
[65] Q. Wen, D. Yan, F. Liu, M. Wang, Y. Ling, P. Wang, P. Kluth, D. Schauries, C. Trautmann, P. Apel, Highly selective ionic transport through subnanometer pores in polymer films, Adv. Funct. Mater. 26 (2016) 5796–5803.
[66] M. Tagliazucchi, I. Szleifer, Chemically Modified Nanopores and Nanochannels, William Andrew, 2016.
[67] F.T. Acar, S.F. Buchsbaum, C. Combs, F. Fornasiero, Z.S. Siwy, Biomimetic potassium-selective nanopores, Sci. Adv. 5 (2019) eaav2568, https://doi.org/10.1126/sciadv.aav2568.
[68] Y. Chen, Y. Zhu, Y. Ruan, N. Zhao, W. Liu, W. Zhuang, X. Lu, Molecular insights into multilayer 18-crown-6-like graphene nanopores for K+/Na+ separation: a molecular dynamics study, Carbon 144 (2019) 32–42, https://doi.org/10.1016/j.carbon.2018.11.048.
[69] S. Balme, J.-M. Janot, L. Berardo, F. Henn, D. Bonhenry, S. Kraszewski, F. Picaud, C. Ramseyer, New bioinspired membrane made of a biological ion channel confined into the cylindrical nanopore of a solid-state polymer, Nano Lett. 11 (2011) 712–716, https://doi.org/10.1021/nl103841m.
[70] S. Balme, F. Picaud, S. Kraszewski, P. Déjardin, J.M. Janot, M. Lepoitevin, J. Capomanes, C. Ramseyer, F. Henn, Controlling potassium selectivity and proton blocking in a hybrid biological/solid-state polymer nanoporous membrane, Nanoscale 5 (2013) 3961–3968, https://doi.org/10.1039/C3NR00564J.
[71] H. Zhang, J. Hou, Y. Hu, P. Wang, R. Ou, L. Jiang, J.Z. Liu, B.D. Freeman, A.J. Hill, H. Wang, Ultrafast selective transport of alkali metal ions in metal organic frameworks with subnanometer pores, Sci. Adv. 4 (2018) eaaq0066.
[72] V.N. Shah, B. Chagot, W.J. Chazin, Calcium-dependent regulation of ion channels, Calcium Bind. Proteins 1 (2006) 203.
[73] D. Voet, J.G. Voet, C.W. Pratt, Fundamentals of Biochemistry, Wiley, New York, 1999.
[74] K. Mason, J. Losos, S. Singer, P. Raven, G. Johnson, Biology, ninth ed., McGraw-Hill, 2011.
[75] T. Balla, Z. Szentpetery, Y.J. Kim, Phosphoinositide signaling: new tools and insights, Physiology 24 (2009) 231–244.
[76] M. Ali, M.N. Tahir, Z. Siwy, R. Neumann, W. Tremel, W. Ensinger, Hydrogen peroxide sensing with horseradish peroxidase-modified polymer single conical nanochannels, Anal. Chem. 83 (2011) 1673–1680.
[77] G. Pérez-Mitta, A.S. Peinetti, M.L. Cortez, M.E. Toimil-Molares, C. Trautmann, O. Azzaroni, Highly sensitive biosensing with solid-state nanopores displaying enzymatically reconfigurable rectification properties, Nano Lett. 18 (2018) 3303–3310, https://doi.org/10.1021/acs.nanolett.8b01281.
[78] P.H. Tse, D.A. Gough, Time-dependent inactivation of immobilized glucose oxidase and catalase, Biotechnol. Bioeng. 29 (1987) 705–713.
[79] H. Dai, Y. Li, Y. Fu, Y. Li, Enzyme catalysis induced polymer growth in nanochannels: a new approach to regulate ion transport and to study enzyme kinetics in nanospace, Electroanalysis 30 (2018) 328–335.
[80] Y. Chen, D. Zhou, Z. Meng, J. Zhai, An ion-gating multinanochannel system based on a copper-responsive self-cleaving DNAzyme, Chem. Commun. 52 (2016) 10020–10023.
[81] D. Han, L.P. Zaino, K. Fu, P.W. Bohn, Redox cycling in nanopore-confined recessed dual-ring electrode arrays, J. Phys. Chem. C 120 (2016) 20634–20641, https://doi.org/10.1021/acs.jpcc.6b01287.
[82] C. Ma, W. Xu, W.R.A. Wichert, P.W. Bohn, Ion accumulation and migration effects on redox cycling in nanopore electrode arrays at low ionic strength, ACS Nano 10 (2016) 3658–3664, https://doi.org/10.1021/acsnano.6b00049.
[83] Y.-L. Ying, Y.-X. Hu, R. Gao, R.-J. Yu, Z. Gu, L.P. Lee, Y.-T. Long, Asymmetric nanopore electrode-based amplification for electron transfer imaging in live cells, J. Am. Chem. Soc. 140 (2018) 5385–5392.
[84] C. Dekker, Solid-state nanopores, Nat. Nanotechnol. 2 (2007) 209.
[85] H. Bayley, Nanopore sequencing: from imagination to reality, Clin. Chem. 61 (2015) 25–31, https://doi.org/10.1373/clinchem.2014.223016.
[86] D. Branton, D.W. Deamer, A. Marziali, H. Bayley, S.A. Benner, T. Butler, M. Di Ventra, S. Garaj, A. Hibbs, X. Huang, S.B. Jovanovich, P.S. Krstic, S. Lindsay, X.S. Ling, C.H. Mastrangelo, A. Meller, J.S. Oliver, Y.V. Pershin, J.M. Ramsey, R. Riehn, G.V. Soni, V.T. Cossa, M. Wanunu, M. Wiggin, J.A. Schloss, The potential and challenges of nanopore sequencing, in: Nanosci. Technol., Macmillan Publishers Ltd., UK, 2009, pp. 261–268, https://doi.org/10.1142/9789814287005_0027.
[87] M. Jain, H.E. Olsen, B. Paten, M. Akeson, The Oxford Nanopore MinION: delivery of nanopore sequencing to the genomics community, Genome Biol. 17 (2016) 239.
[88] N.A.W. Bell, M. Muthukumar, U.F. Keyser, Translocation frequency of double-stranded DNA through a solid-state nanopore, Phys. Rev. E. 93 (2016), 022401, https://doi.org/10.1103/PhysRevE.93.022401.
[89] S.J. Heerema, L. Vicarelli, S. Pud, R.N. Schouten, H.W. Zandbergen, C. Dekker, Probing DNA translocations with inplane current signals in a graphene nanoribbon with a nanopore, ACS Nano 12 (2018) 2623–2633, https://doi.org/10.1021/acsnano.7b08635.
[90] G. Danda, P. Masih Das, Y.-C. Chou, J.T. Mlack, W.M. Parkin, C.H. Naylor, K. Fujisawa, T. Zhang, L.B. Fulton, M. Terrones, A.T.C. Johnson, M. Drndić, Monolayer WS2 nanopores for DNA translocation with light-adjustable sizes, ACS Nano 11 (2017) 1937–1945, https://doi.org/10.1021/acsnano.6b08028.
[91] H. Wu, Y. Chen, Q. Zhou, R. Wang, B. Xia, D. Ma, K. Luo, Q. Liu, Translocation of rigid rod-shaped virus through various solid-state nanopores, Anal. Chem. 88 (2016) 2502–2510, https://doi.org/10.1021/acs.analchem.5b04905.
[92] M.S. Rodriguez, C. Dargemont, F. Stutz, Nuclear export of RNA, Biol. Cell. 96 (2004) 639–655, https://doi.org/10.1016/j.biolcel.2004.04.014.
[93] M. Tagliazucchi, O. Peleg, M. Kröger, Y. Rabin, I. Szleifer, Effect of charge, hydrophobicity, and sequence of nucleoporins on the translocation of model particles through the nuclear pore complex, Proc. Natl. Acad. Sci. 110 (2013) 3363–3368, https://doi.org/10.1073/pnas.1212909110.
[94] L.J. Colwell, M.P. Brenner, K. Ribbeck, Charge as a selection criterion for translocation through the nuclear pore complex, PLoS Comput. Biol. 6 (2010), https://doi.org/10.1371/journal.pcbi.1000747 e1000747.

C. Trautmann, Ultrafast ion sieving using nanoporous polymeric membranes, Nat. Commun. 9 (2018) 569.
[65] Q. Wen, D. Yan, F. Liu, M. Wang, Y. Ling, P. Wang, P. Kluth, D. Schauries, C. Trautmann, P. Apel, Highly selective ionic transport through sub-nanometer pores in polymer films, Adv. Funct. Mater. 26 (2016) 5796–5803.
[66] M. Tagliazucchi, I. Szleifer, Chemically Modified Nanopores and Nano-
88 (2016) 2502–2510, https://doi.org/10.1021/acs.analchem.5b04905.
[92] M.S. Rodriguez, C. Dargemont, F. Stutz, Nuclear export of RNA, Biol. Cell. 96 (2004) 639–655, https://doi.org/10.1016/j.biolcel.2004.04.014.
[93] M. Tagliazucchi, O. Peleg, M. Kröger, Y. Rabin, I. Szleifer, Effect of charge, hydrophobicity, and sequence of nucleoporins on the translocation of model particles through the nuclear pore complex, Proc. Natl. Acad. Sci. 110 (2013)

[95] L.E. Kapinos, R.L. Schoch, R.S. Wagner, K.D. Schleicher, R.Y. Lim, Karyopherin-centric control of nuclear pores based on molecular occupancy and kinetic analysis of multivalent binding with FG nucleoporins, Biophys. J. 106 (2014) 1751–1762.
[96] S.W. Kowalczyk, L. Kapinos, T.R. Blosser, T. Magalhães, P. van Nies, R.Y.H. Lim, C. Dekker, Single-molecule transport across an individual biomimetic nuclear pore complex, Nat. Nanotechnol. 6 (2011) 433–438, https://doi.org/10.1038/nnano.2011.88.
[97] T. Jovanovic-Talisman, J. Tetenbaum-Novatt, A.S. McKenney, A. Zilman, R. Peters, M.P. Rout, B.T. Chait, Artificial nanopores that mimic the transport selectivity of the nuclear pore complex, Nature 457 (2009) 1023–1027, https://doi.org/10.1038/nature07600.
[98] G. Emilsson, Y. Sakiyama, B. Malekian, K. Xiong, Z. Adali-Kaya, R.Y.H. Lim, A.B. Dahlin, Gating protein transport in solid state nanopores by single molecule recognition, ACS Cent. Sci. 4 (2018) 1007–1014, https://doi.org/10.1021/acscentsci.8b00268.
[99] A.N. Ananth, A. Mishra, S. Frey, A. Dwarkasing, R. Versloot, E. van der Giessen, D. Görlich, P. Onck, C. Dekker, Spatial structure of disordered proteins dictates conductance and selectivity in nuclear pore complex mimics, Elife 7 (2018) e31510.
[100] P. Ketterer, A.N. Ananth, D.S.L. Trip, A. Mishra, E. Bertosin, M. Ganji, J. van der Torre, P. Onck, H. Dietz, C. Dekker, DNA origami scaffold for studying intrinsically disordered proteins of the nuclear pore complex, Nat. Commun. 9 (2018) 1–8, https://doi.org/10.1038/s41467-018-03313-w.
[101] K. Huang, I. Szleifer, Design of multifunctional nanogate in response to multiple external stimuli using amphiphilic diblock copolymer, J. Am. Chem. Soc. 139 (2017) 6422–6430, https://doi.org/10.1021/jacs.7b02057.
[102] M. Tagliazucchi, K. Huang, I. Szleifer, Routes for nanoparticle translocation through polymer-brush-modified nanopores, J. Phys. Condens. Matter 30 (2018) 274006, https://doi.org/10.1088/1361-648X/aac90b.
[103] R. Zwanzig, Diffusion in a rough potential, Proc. Natl. Acad. Sci. 85 (1988) 2029–2030.
[104] R. Karnik, R. Fan, M. Yue, D. Li, P. Yang, A. Majumdar, Electrostatic control of ions and molecules in nanofluidic transistors, Nano Lett. 5 (2005) 943–948.